

Cooperative Phagocytes

Resident Microglia and Bone Marrow Immigrants Remove Dead Photoreceptors in Retinal Lesions

Sandrine Joly,* Mike Francke,[†] Elke Ulbricht,[†]
Susanne Beck,[‡] Matthias Seeliger,[‡]
Petra Hirrlinger,[†] Johannes Hirrlinger,[§] Karl S. Lang,[¶]
Martin Zinkernagel,^{||} Bernhard Odermatt,^{**}
Marijana Samardzija,* Andreas Reichenbach,[†]
Christian Grimm,* and Charlotte E. Remé*

From the Laboratory for Retinal Cell Biology,* Department of Ophthalmology, University of Zurich, Zurich, Switzerland; the Paul-Flechsig-Institute for Brain Research,[†] University of Leipzig, Leipzig, Germany; the Ocular Neurodegeneration Research Group,[‡] Centre for Ophthalmology, Institute for Ophthalmic Research, University of Tuebingen, Tuebingen, Germany; the Interdisciplinary Centre for Clinical Research,[§] N05-Neural Plasticity, Leipzig, Germany; the Institutes of Experimental Immunology[¶] and Pathology,^{**} University Hospital of Zurich, Zurich, Switzerland; and the Research Department,^{||} Kantonale Hospital of St. Gallen, Gallen, Switzerland

Phagocytosis is essential for the removal of photoreceptor debris following retinal injury. We used two mouse models, mice injected with green fluorescent protein-labeled bone marrow cells or green fluorescent protein-labeled microglia, to study the origin and activation patterns of phagocytic cells after acute blue light-induced retinal lesions. We show that following injury, blood-borne macrophages enter the eye via the optic nerve and ciliary body and soon migrate into the injured retinal area. Resident microglia are also activated rapidly throughout the entire retina and adopt macrophage characteristics only in the injured region. Both blood-borne- and microglia-derived macrophages were involved in the phagocytosis of dead photoreceptors. No obvious breakdown of the blood-retinal barrier was observed. *Ccl4*, *Ccl12*, *Tgfb1*, *Csf1*, and *Tnf* were differentially expressed in both the isolated retina and the eyecup of wild-type mice. Debris-laden macrophages appeared to leave the retina into the general circulation, suggesting their potential to become antigen-presenting cells. These experiments provide evidence that both local and immigrant macrophages

remove apoptotic photoreceptors and cell debris in the injured retina. (Am J Pathol 2009, 174:2310–2323; DOI: 10.2353/ajpath.2009.090023)

Acute light-induced retinal degeneration is characterized by apoptosis of photoreceptor cells and by conspicuous phagocytic cells in the region of cell death.^{1,2} Phagocytic cells are also found in inherited dystrophies, but to a lesser degree at any given time point due to the protracted course of those diseases. The immune privileged status of the retina, similar to the brain, is thought to limit the exit of local and entry of systemic immune cells through the blood-retinal barrier.^{3,4} Nevertheless, a distinct cellular response with phagocytosis of disrupted photoreceptor outer segments and apoptotic cells occurs after acute light-induced degeneration.^{5,6} The origin of such phagocytes can potentially derive from two sources: from blood-borne macrophages or from resident retinal microglia. To track macrophage infiltration from the systemic circulation, green fluorescent protein (GFP)-tagged bone marrow precursor cells were visualized after grafting into lethally irradiated mice.⁷ The fractalkine receptor (CX3CR1) is expressed on central nervous system (CNS) microglia. Microglial cells expressing GFP under the *Cx3cr1* promoter⁸ were used to visualize resident microglia after retinal injury.

Supported by the Swiss National Science Foundation (3100A0-105793 and 3100A0-117760), the Vontobel Foundation, and the German Research Council DFG grants Se 837/5-2, Se 837/6-1 and Se 837/7-1.

Accepted for publication March 5, 2009.

Current address of M.F.: Biological and Soft Systems, Physics Department BSS, University of Cambridge, Cambridge, United Kingdom; K.S.L.: Humboldt Research Group, Department of Gastroenterology, Hepatology and Infectiology, Heinrich Heine University, Düsseldorf, Germany; M.Z.: Lions Eye Institute, Experimental Immunology, Centre for Ophthalmology and Visual Sciences, University of Western Australia, Nedlands, Western Australia.

Address reprint requests to Charlotte E. Remé or Sandrine Joly, Laboratory for Retinal Cell Biology, Department of Ophthalmology, University of Zurich, Frauenklinikstr. 24, 8091 Zurich, Switzerland. E-mail: chreme@ophth.uzh.ch or sandrine.joly@usz.ch.

Inherited retinal dystrophies and age-related macular degeneration are accompanied by glia activation.⁹ Retinal microglia, as brain microglia,^{10,11} can promote photoreceptor death¹² but can also be protective^{13,14} depending on the experimental conditions. Activated microglia and hematogenous macrophages might increase damage by releasing inflammatory cytokines and chemokines and trigger the formation of toxic molecules such as nitric oxide, reactive oxygen species and free radicals, collectively called molecules of oxidative stress.¹⁰ Protection may be achieved by the release of neuroprotective messengers.¹³

To date, the cellular and molecular mechanisms of microglia activation and the function in acute and chronic degeneration have not been elucidated in detail for the retina. Moreover, the relative proportion of blood-borne macrophages and of resident microglia recruited to clean the retina from dead photoreceptors has never been investigated so far. Here we show for the acutely injured retina that bone marrow-derived cells rapidly immigrate through the vascular system of the ciliary body and optic nerve and differentiate into macrophages. We demonstrate that resident retinal microglia is activated as well and both hematogenous cells and retinal microglia participate in the phagocytosis of destroyed photoreceptor cells. *In vivo* monitoring by scanning laser ophthalmoscopy (SLO) and indocyanine green angiography of acute-phase lesions showed immigrating blood cells without major disruption of the blood-retinal barrier. Electron microscopy indicated the exit of debris-laden macrophages into the general circulation.

Inflammatory processes have recently been recognized to contribute to the pathogenesis of age-related macular degeneration and glaucoma, diseases that were previously considered mainly degenerative.¹⁵⁻¹⁷ Moreover, several cytokines and chemokines were identified to be involved in the activation process of macrophages and microglial cells in brain and retina, respectively, such as fractalkine, *Tnf*, *Ccl4*, *Ccl2*, and stromal-derived factor 1.^{14,18,19} However, these strongly regulated processes are poorly understood to date and may differ significantly in different organs²⁰ or under different conditions in the same organ. Therefore, we investigated several pro- and anti-inflammatory cytokines and chemokines and found differing patterns of up-regulation in the isolated retina and eyecup in wild-type mice. Inflammatory messengers are localized specifically in macrophages within the area of damage but not in retinal neurons or Müller cells.

Materials and Methods

Animals

All procedures were performed in accordance with the Association for Research in Vision and Ophthalmology statement for the use of animals in ophthalmic and vision research and within the guidelines of the Cantonal Veterinary Authorities of Zurich. One day after lethal irradiation (950 rad), young recipient C57BL/6 mice were transplanted by intravenous injection of 8×10^6 bone marrow

cells, generated by flushing the femur and tibia of C57BL/6 donor mice carrying the green fluorescent protein (GFP^{+/+}) gene under the chicken β -actin promoter.⁷ Light exposure was performed 6 to 8 weeks after transplantation. We also used transgenic heterozygous and homozygous mice where the fractalkine receptor gene (CX3CR1) was replaced by GFP (CX3CR1^{+/-}; CX3CR1^{-/-}).⁸ Control mice were age-matched wild-type C57BL/6 mice obtained from the Central Biological Laboratory of the University of Zurich.

Light Exposure of Mice

Exposure to blue light has been previously described.²¹ For this study, improvements of the optical system were introduced, guiding the light under Maxwellian view into the eye with a spot of 5 mm² focused on the cornea. When an irradiance of 30 mW/cm² was measured at the corneal focus, the retinal irradiance within the "hot spot" was about 62 mW/cm² with blue light bandwidth of 410 ± 10 nm. The photon flux calculated was 6.2×10^9 photons $\mu\text{m}^{-2} \text{s}^{-1}$ at 410 nm. The rate of rhodopsin isomerizations was $1.45 \times 10^9 \text{s}^{-1}$ at 410 nm.²²

Mice were dark-adapted for 12 hours and pupils were dilated with cyclogyl 1% (Alcon Pharmaceuticals, Hünenberg, Switzerland) and phenylephrine 5% (Bausch & Lomb Swiss AG, Steinhausen, Switzerland) in dim red light 30 minutes before anesthesia. Anesthesia consisted of a mixture of ketamine (75 mg/kg) (Parke Davis, Switzerland), xylazine 2% (23 mg/kg) (Bayer AG, Leverkusen), and sodium chloride. For light exposure, mice were placed in a special holder where their heads and eyes could be adjusted to the light beam, the distance from the cornea was 1 cm. The cornea was kept moist with a drop of Methocel 2% (OmniVision AG, Neuhausen, Switzerland) during the duration of the experiment (2 minutes of blue light/eye). With this method, a reproducible, central focus of light-induced lesions termed "hot spot" was achieved. Mice were sacrificed at 6 hours, 12 hours, 24 hours, 3 days, 6 days, 10 days, 5 weeks, and 10 weeks, respectively, after light exposure.

In Vivo Monitoring by SLO and Indocyanine Green Angiography

Twenty-four hours after blue light exposure, bone marrow chimeric (BMC) mice and controls were observed by SLO. Mice were anesthetized with ketamine (66.7 mg/kg) and xylazine (11.7 mg/kg) and the pupils were dilated with tropicamide eye drops (Mydriaticum Stulln, Pharma Stulln, Stulln, Germany). SLO imaging was performed with a Heidelberg retina angiograph (HRA I, Heidelberg Engineering, Germany), a confocal scanning-laser ophthalmoscope according to previously reported procedures.²³ Briefly, the HRA features two argon wavelengths (488 nm and 514 nm) in the short wavelength range and two infrared diode lasers (795 nm and 830 nm) in the long wavelength range. The confocal diaphragm of the SLO allows visualizing different planes of the posterior pole, ranging from the inner surface of the retina down to the

Table 1. List of Antibodies Used for Fluorescence Microscopy

Antibody name	Type	Dilution	Source	Catalog number	Cell type detection
Isolectin GS-IB4	<i>Griffonia simplicifolia</i>	1:50	Invitrogen	I21413	Microglia, blood vessels
Iba-1	rAb	1:1000	Wako	019-19741	Microglia and macrophages
CD68 (ED1)	mAb	1:100	Chemicon	MAB1435	Activated macrophages
Rhodopsin (Rho4D2)	mAb	1:100	David Hicks	See Ref. 56	Rod outer segment
CCL5	mAb	1:20	R&D Systems	IC278P	
TNF	mAb	1:13	R&D Systems	AF-410NA	

retinal pigment epithelium and the choroid. To detect possible effects of blue light exposure on the vascular system, angiography was performed using the 795 nm laser wavelength after a subcutaneous injection of 50 mg/kg body weight indocyanine green (ICG-Pulsion, Pulsion Medical Systems AG, Munich, Germany).

Immunofluorescence Microscopy

Mice were perfused intracardially and immunohistochemistry was performed as previously described.⁶ After blocking, different primary antibodies were applied on sections and kept overnight in a humid chamber at 4°C (Table 1). Secondary antibodies labeled with Cy3 were used (Jackson ImmunoResearch, West Grove, PA). Stainings were examined with an Axioplan2 microscope (Carl Zeiss, Jena, Germany) using a 10× (numerical aperture 0.45) or a 20× (numerical aperture 0.50) magnification. Pictures were taken with a digital imaging system (AxioCam, Carl Zeiss, Jena, Germany). In both strains, GFP autofluorescence was directly visualized without additional staining.

For confocal laser scanning microscopy (LSM 510, Zeiss, Oberkochen, Germany), perfused eyecups were flat mounted on a glass slide, coverslipped and examined at different wavelengths (488 nm, 543 nm, and 633 nm). Analysis of the microglial cell processes in the CX3CR1^{-/-} mice was performed with an upright confocal two-photon laser scanning microscope (Zeiss LSM 510NLO; Axioskop FS2M, Zeiss, Oberkochen, Germany) with Chameleon laser (Coherent, Dieburg, Germany) and C-Apochromat 40x/1.2NA water immersion objective. GFP fluorescence was excited at 890 nm (infrared); emission was recorded at 500–550 nm (green) band-pass filter and non-descanned detection. Three-dimensional image stacks with x-y frame sizes of 1024 × 1024 pixels (voxel size of 0.29 × 0.29 × 1 μm) were recorded spanning the whole thickness of the retina. Three-dimensional

reconstructions were calculated using the Zeiss LSM image software and the number of microglia cells and process length in the outer retinal layers were analyzed. For the number of microglial cells and processes, the statistical analysis was performed using the nonparametric Mann Whitney rank sum test (*U*-test) (*N* = 9; ***P* < 0.01).

Electron Microscopy

Mice were euthanized by cervical dislocation. The eyes were removed, fixed in 2.5% glutaraldehyde in 0.1 mol/L cacodylate buffer overnight and the central retina was trimmed, washed, dehydrated, and Epon-embedded. Ultrathin sections were stained with uranyl acetate and lead citrate and observed with a Phillips CM12 (1990) electron microscope.

RNA Isolation, Reverse Transcription, and Quantitative Real-Time Polymerase Chain Reaction

Mice were sacrificed under dim red light after dark adaptation or at 6 hours, 12 hours, 24 hours, or 3 days after light exposure. Retinas were removed through a slit in the cornea and the corresponding eyecups (retinal pigment epithelium, choroid, sclera) were prepared (*n* = 6 for dark controls, *n* = 3 for light-exposed specimens), immediately frozen in liquid nitrogen and stored at -80°C until further use. RNA isolation from retinas, cDNA synthesis and gene expression analysis were performed as previously described.²⁴ Primer pairs used for specific amplifications were designed to span intronic sequences or cover exon-intron boundaries (Table 2). mRNA levels were normalized to β-actin for relative quantification of gene expression. Each reaction was done in duplicate. Statistical analysis was performed using a one-way anal-

Table 2. PCR Primers Used for Real-Time Polymerase Chain Reaction Amplification

Genes	Upstream	Downstream	Product size
<i>β-actin</i>	5'-CAACGGCTCCGGCATGTGC-3'	5'-CTCTTGCTCTGGCCTCG-3'	153 bp
<i>Ccl4</i>	5'-CAAGCCAGCTGTGGTATTC-3'	5'-AGCTGCTCAGTTCACCTCC-3'	109 bp
<i>Ccl12</i>	5'-CCTCAGGTATTGGCTGGAC-3'	5'-GACACTGGCTGCTTGTGATT-3'	124 bp
<i>Ccl5</i>	5'-GCTCCAATCTTGCAGTCGT-3'	5'-CTAGAGCAAGCGATGACAGG-3'	165 bp
<i>Ccl9</i>	5'-CAACTGCTCTTGGAACTCTGG-3'	5'-AGGCAGCAATCTGAAGAGTC-3'	136 bp
<i>Csf1</i>	5'-GCTCCAGGAAGCTTCCAAATA-3'	5'-TCTTGATCTTCTCCAGCAGC-3'	119 bp
<i>Tnf</i>	5'-CCACGCTCTTCTGTCTACTGA-3'	5'-GGCCATAGAAGCTGATGAGAGG-3'	92 bp
<i>Tgfb1</i>	5'-GCAACATGTGGAAGCTTACCAG-3'	5'-CAGCCACTCAGGCGTATCA-3'	94 bp

ysis of variance (analysis of variance) followed by a Tukey post hoc test (GraphPad Software, Inc.).

Results

Confocal SLO in BMC and Control Mice

To monitor the state of the blood-retinal barrier and to establish the involvement of blood-borne macrophages migrating into the retinal injury site *in vivo*, we used BMC mice that were lethally irradiated and transplanted with GFP-expressing bone marrow cells. The ocular fundus (excitation at 514 nm), fundus autofluorescence (excitation at 488 nm and 795 nm) and indocyanine green angiography (excitation at 795 nm) was monitored by SLO in wild-type control and BMC mice 1, 7, and 14 days after blue light exposure (Figure 1). No leakage of retinal vessels was apparent at different time points in control and BMC mice, indicating that no major breakdown of the blood-retinal barrier occurred (Figure 1C).

At 514 nm funduscopy, a circumscribed area in the ocular fundus, previously termed hot spot,²¹ was easily detectable in retinas of control and BMC mice 1 day after blue light exposure (Figure 1A, arrows). The hot spot, which appears lighter than the remaining retina in the 514-nm funduscopy, masked the choroidal vasculature and is likely due to a subretinal fluid accumulation. At all time points analyzed, no major difference in the fundus imaging was observed between control and BMC mice (Figure 1B and 1C). At an excitation of 488 nm, fundus examination revealed the presence of GFP-positive autofluorescent bone marrow cells in vessels and retinal tissue of BMC mice 1 day after light (Figure 1A, star). No autofluorescence was detected in control wild-type mice. Autofluorescent cells remained in the retina of BMC mice until the end of the observation period (Figure 1, B, and C, star). In both control and BMC mice we observed an accumulation of autofluorescent material within the hot spot area at both excitation wavelengths (488 nm and 795 nm) at 7 and 14 days (Figure 1B and 1C, arrowheads). These findings suggest that retinoid-containing debris with the corresponding absorption of 488 nm and debris of to date unknown molecular composition with an absorption of 795 nm accumulate within the hot spot region (subretinal space and pigment epithelium). Retinoids are contained in breakdown products of photoreceptor outer segments that contain the visual pigment chromophore 11-*cis*-retinal. In addition, however, macrophages having engulfed photoreceptor material may still be present in the hot spot region.

Blood-Borne Macrophages Invade Specifically the Injured Side of the Retina in BMC Mice after Blue Light Exposure

To localize and to identify blood-borne macrophages, GFP autofluorescence was observed on retinal cryosections alone or combined with antibodies for microglia (GSA-IB4 and Iba1) or macrophages (Iba1 and CD68)

(Figure 2). Unexposed retinas from BMC mice presented green fluorescent cells within choroidal and conjunctival blood vessels, within presumptive meninges and connective tissues around the optic nerve (Figure 2A, left panel) but not in the retina itself. Only few cells appeared in retinal vessels, whereas the regions of the ciliary body and overlying conjunctiva were more populated (Figure 2B, left panel, arrows). Three days after light exposure, the optic nerve head and the ciliary body were strongly colonized by green bone marrow cells (Figure 2, A, B, arrow, right panels). The migration of green bone marrow cells was more pronounced into the area of the hot spot (Figure 2A, right panel, arrow) than in the contralateral side that underwent no damage in the light-exposed eye (Figure 2A, right panel, arrowhead).

Immunofluorescence was performed on retinal tissues to identify blood-borne macrophages that may or may not express glia markers. In BMC mice, the hot spot region revealed different cell populations 3 and 6 days after light exposure, respectively (Figure 2C): 1) green fluorescent macrophages only expressing the GFP protein; 2) GFP-expressing macrophages additionally stained with one of the glia markers GSA-IB4 or Iba1 (yellow); and 3) a minority of cells expressing only glia markers (red). Staining of GFP cells (green) with anti-CD68 (red) confirmed the presence of activated macrophages in the hot spot zone of BMC retinas 6 days after exposure (Figure 2D). These different expression patterns were only seen within the hot spot region but not in the contralateral side of the light-exposed eye and indicate different populations of macrophages with and without microglial characteristics, respectively. At 5 and 10 weeks after exposure, the retina showed a "scar" in the area of the hot spot with loss of photoreceptors and remaining fluorescent cells within the vasculature of the posterior eye (data not shown). Around the optic nerve head, distinct green cell populations were seen throughout the entire observation period up to 10 weeks (data not shown).

GFP Fluorescent Microglial Cells Adopt Macrophage Characteristics in the Hot Spot Region, While Microglia on the Contralateral Side Is Activated but Not Phagocytic in CX3CR1^{-/-} Mouse Retina

CX3CR1^{-/-} knockout mice express GFP instead of CX3CR1 and specifically label microglia.⁸ GFP-fluorescent microglial cells of unexposed control mice showed an even distribution throughout the entire retina (Figure 3A, left panel). Three days after light exposure, retinas displayed massive accumulation of green cells in the optic nerve and in the hot spot region similar to BMC mice (Figure 3A, right panel, arrow). Compared with the exposed BMC retina where green cells were absent in the contralateral side of the light-exposed eye, CX3CR1^{-/-} retinas showed microglia in the outer plexiform layer and in the inner plexiform layer that are likely resident (Figure 3A, left panel, arrowhead).

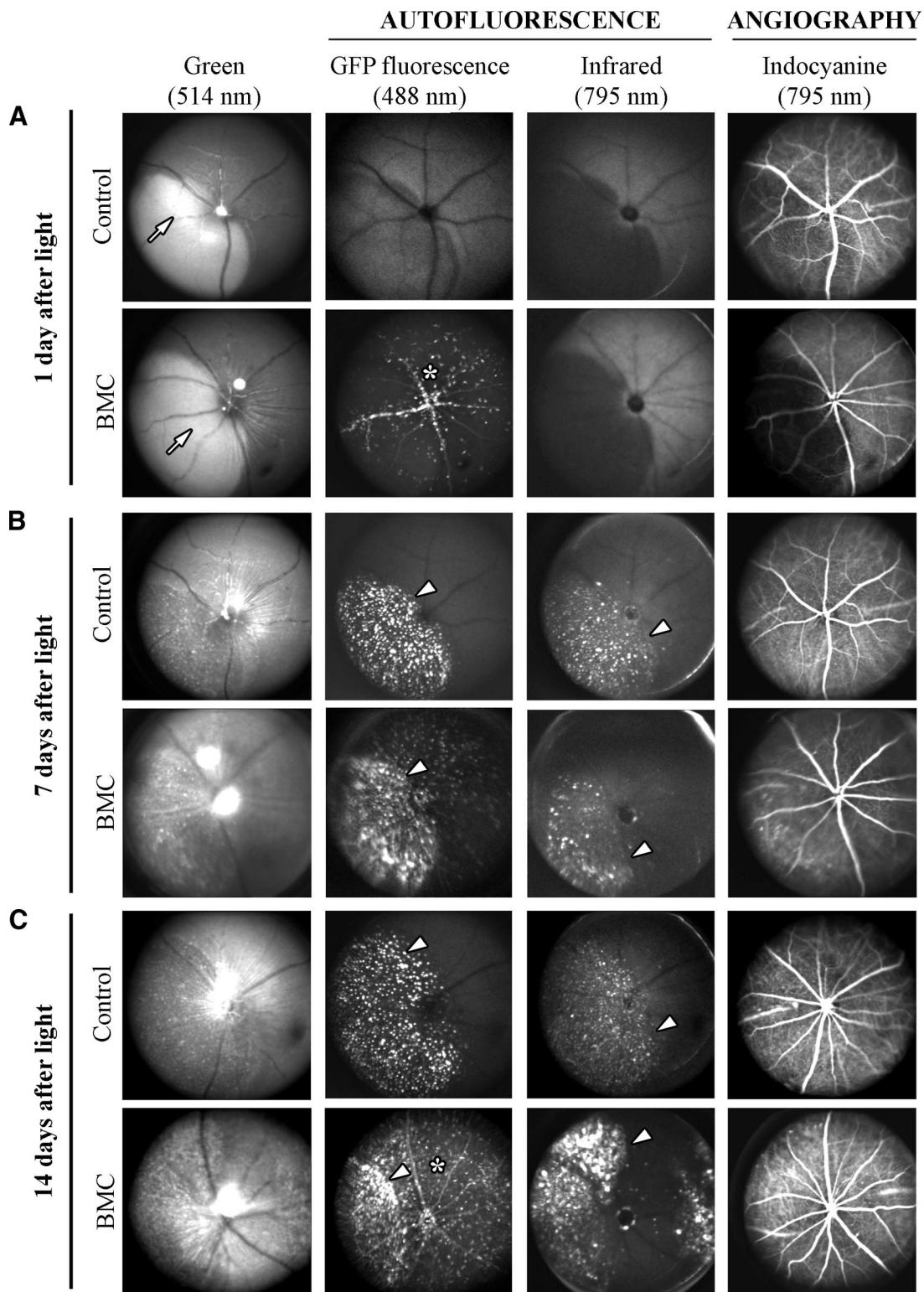


Figure 1. SLO and angiography in BMC and wild-type mice. **A:** One day after light exposure, wild-type (control) and BMC mice showed a subretinal edema in the hot spot (**arrow**), which appeared lighter than the remaining fundus in the 514 nm-funduscopy. Fluorescence of bone marrow-derived cells was distinct within vessels and in retinal tissue (**asterisk**) of BMC mice. Indocyanine green angiography showed no leakage of retinal and choroidal vessels in control and BMC mice. **B:** Seven days after light exposure, in addition to GFP fluorescence of cells in BMC, both control and BMC mice displayed distinct autofluorescent deposits in the hot spot absorbing at 488 and 795 nm (**arrowheads**). **C:** Fourteen days after light exposure, accumulation of retinoid-containing cellular debris in the hot spot region persisted (**arrowheads**) and GFP fluorescent cells were distributed in the entire retina (**asterisk**).

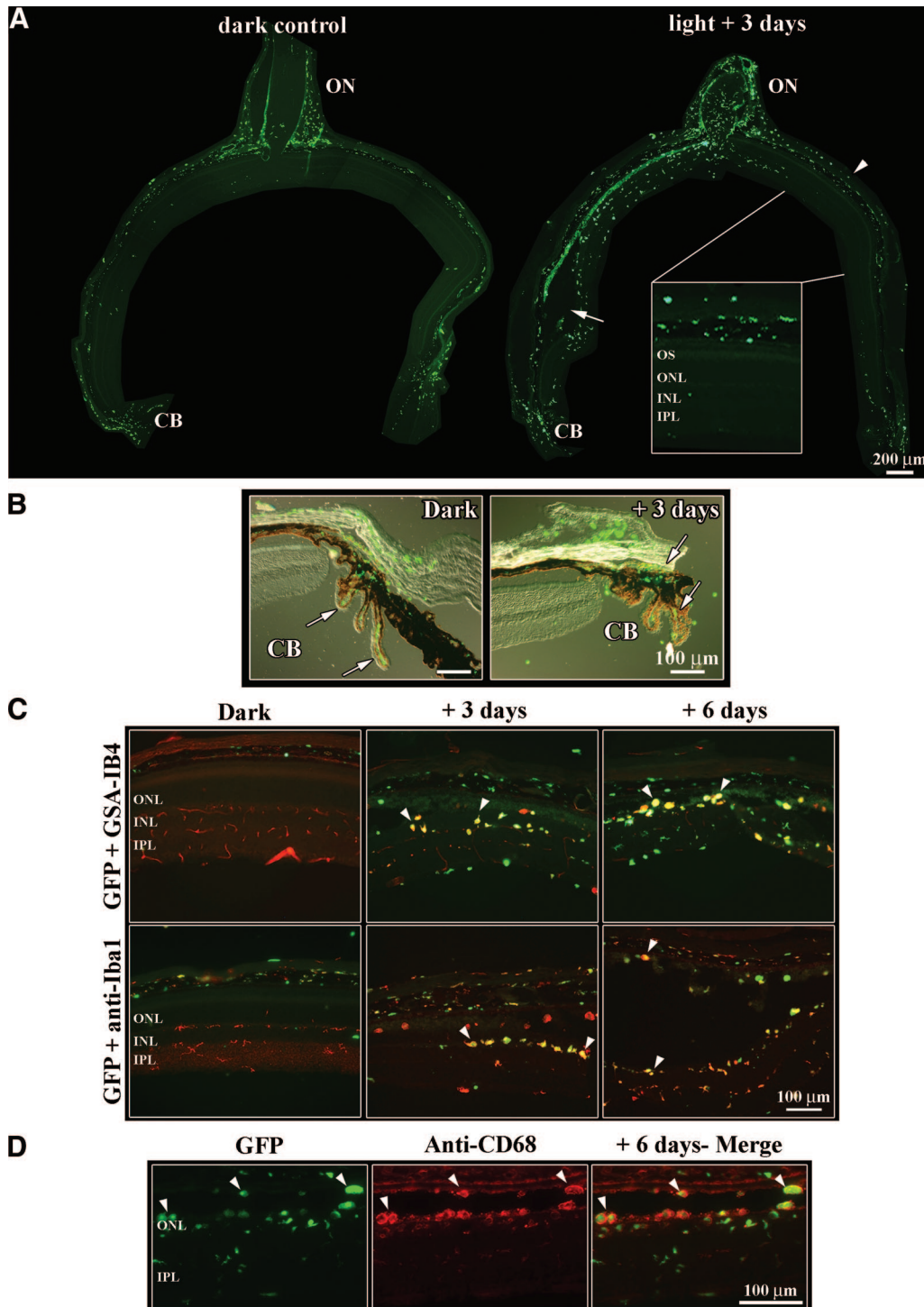


Figure 2. Localization and cell type identification of bone marrow-derived cells in control and light-exposed BMC retinas. **A:** GFP-positive cells were detected by their autofluorescence on retinal cryosections cut through the optic nerve and analyzed by fluorescence microscopy. In dark control retinas, GFP-positive cells were mainly localized within meninges and connective tissues around the optic nerve and in the ciliary body, while the retinal tissue was almost completely lacking green cells (**left**). Three days after exposure (**right**), green cells were accumulating in the hot spot region (**arrow**) whereas in the contralateral retina of the light-exposed eye, GFP-positive cells were limited to the choroid (**arrowhead** and close-up). Scale bar = 200 μ m; 66.7 μ m for **inset**. **B:** Overlay of Nomarski and fluorescent images to show the presence of GFP-positive cells in the ciliary body (CB, **arrows**). **C:** Stainings of BMC retinas with glia markers GSA-IB4 (red, **upper row**) and anti-Iba1 antibodies (red, **lower row**) revealed three distinct populations of labeled cells (red, green and yellow appearance, respectively). Staining with GSA-IB4 lectin labeled additionally all blood vessels in the control (dark) retina (**upper left**). Anti-Iba1 antibodies labeled resident microglial cells in the control retina (red). Yellow appearing round macrophages in the hot spot indicate immigrated bone marrow cells (**arrowheads**). **D:** Fluorescence microscopy of retinal sections revealed a colocalization of GFP-positive cells with CD68, a marker for activated macrophages (**arrowheads**). ON, optic nerve; CB, ciliary body; OS, outer segment; ONL, outer nuclear layer; INL, inner nuclear layer; IPL, inner plexiform layer.

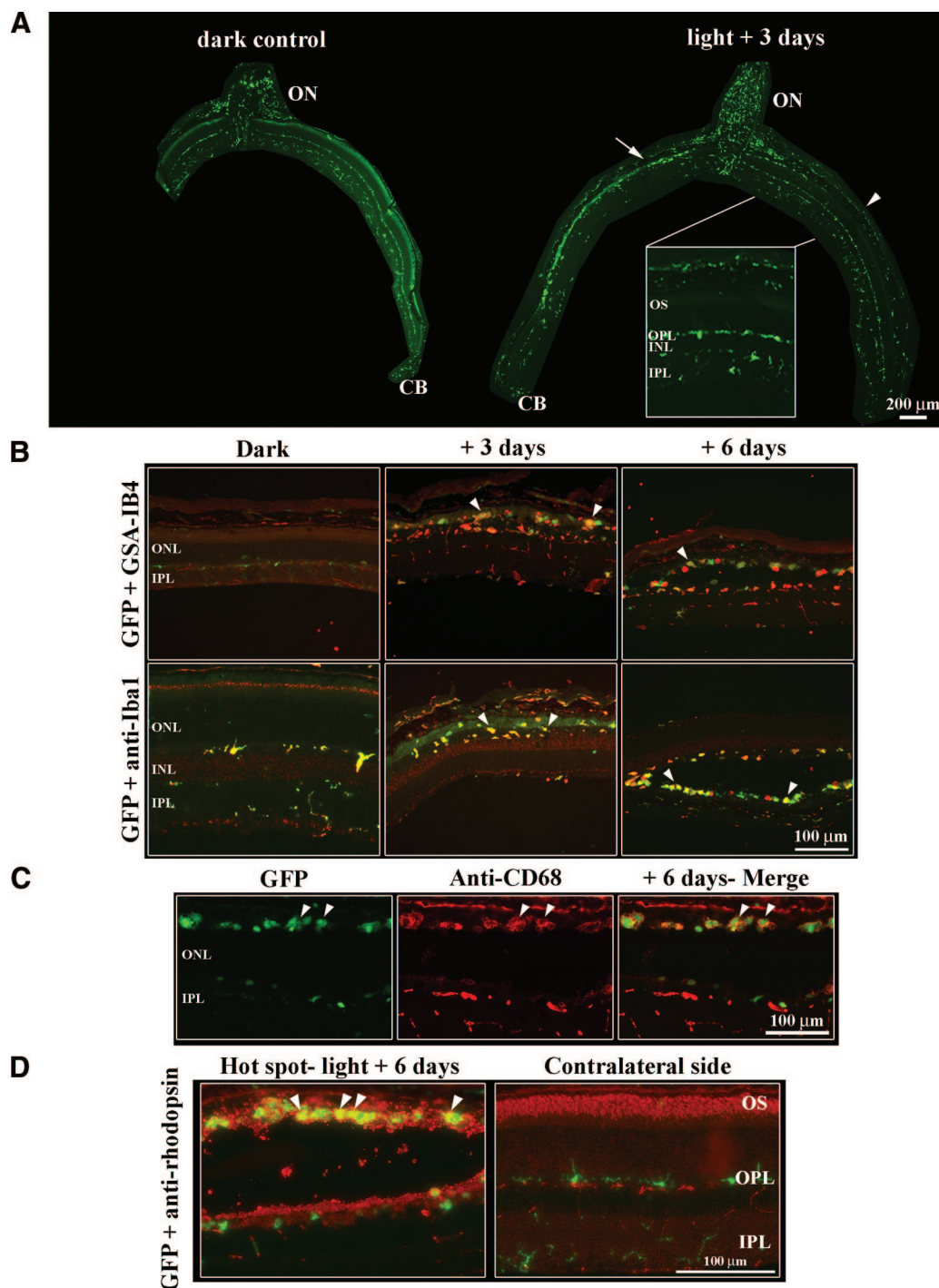


Figure 3. Localization and cell type identification of the GFP-fluorescent microglial cells in control and light-exposed $CX3CR1^{-/-}$ retinas. **A:** In $CX3CR1^{-/-}$ dark control retinas, GFP-autofluorescent microglial cells were mainly localized around the optic nerve head and in the retinal plexiform layers (**left**). Three days after exposure (**right**), microglia was concentrated in the outer retina of the hot spot area (**arrow**) but not in the unaffected retinal parts (**arrowhead**). Note the massive presence of resting microglia in the contralateral uninjured side (in the light-exposed eye) in the plexiform layers (close-up). Scale bar = 200 μm ; 66.7 μm for **inset**. **B:** Staining of $CX3CR1^{-/-}$ retinas with glia markers GSA-IB4 (red, **upper row**) and anti-Iba1 antibodies (red, **lower row**) revealed distinct populations of labeled cells. The GSA-IB4 lectin staining of resting microglial cells is very faint (control, **upper left**) compared with the clear double labeling with anti-Iba1 (**lower left**). Activated microglial cells in the hot spot revealed the round morphology of phagocytes and were clearly labeled by both glial markers (**arrowheads**). **C:** Staining with anti-CD68 for activated macrophages shows labeling of cells in the hot spot region of $CX3CR1^{-/-}$ mice after light exposure (**arrowhead**). **D:** Fluorescence micrographs showing macrophages in the hot spot with distinct staining patterns for rhodopsin (**arrowheads**) in $CX3CR1^{-/-}$ mice. In the contralateral non-damaged region of the light-exposed eye, no macrophages are seen but GFP-positive glia in the OPL and IPL.

Immunostaining with the lectin GSA-IB4 and the anti-Iba1 antibody revealed that microglia was strongly activated 3 and 6 days after light exposure in the hot spot region and showed macrophage morphology (Figure

3B). Similarly to BMC mice, GFP-microglia stained with anti-CD68, a specific marker for activated macrophages, confirmed that retinal glia-derived macrophages populated the hot spot 6 days after exposure (Figure 3C, arrows).

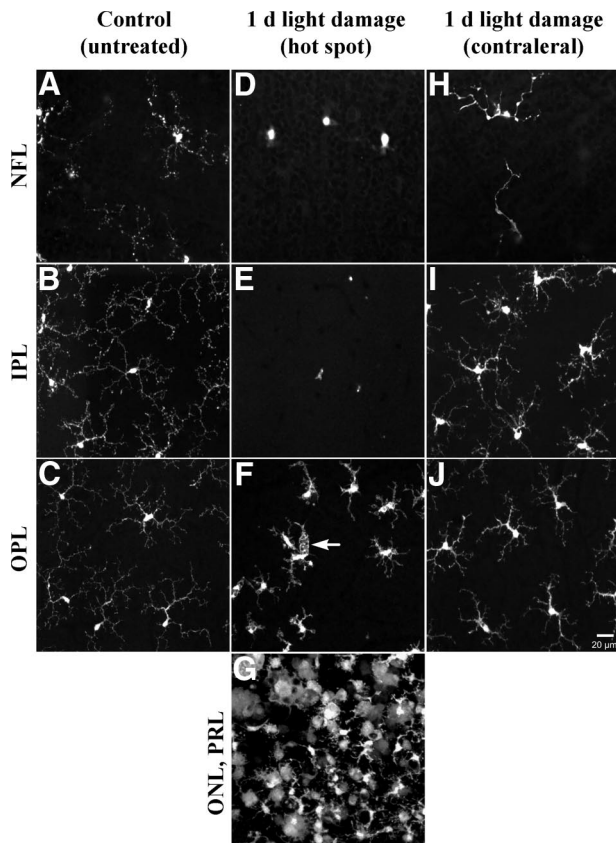


Figure 4. Confocal light micrographs of CX3CR1^{-/-} control retinas and 1 day after light exposure (view onto flat mount retinas at different layers). **A–C:** Microglial cells expressing GFP under control of the Cx3CR1 promoter in the NFL, IPL, and OPL were characterized by small cell bodies and extensive, fine arborizations of their processes. **D–G:** In the hot spot area, a remarkable lack of microglial cells occurred in the NFL and IPL, whereas the OPL showed activated microglia with shortened, thick processes showing initial signs of phagocytosis (**white arrow**) and rounded cell bodies. In the hot spot, microglial cells displayed macrophage-like morphology with some cells still displaying glia-like morphology with thickened processes (**G**). **H–J:** Microglia in the contralateral unexposed retina (from the light-exposed eye) showed already signs of activation in NFL, IPL, and OPL compared with controls. PRL, photoreceptor layer.

Interestingly, 6 days after exposure, GFP-fluorescent microglial cells were located at the level of damage, ie, in the photoreceptor outer segment layer (Figure 3D). The colocalization of microglia-derived macrophages with an anti-rhodopsin antibody (anti-Rho4D2, red) indicated that microglial cells phagocytosed photoreceptor debris (Figure 3D, arrowheads). On the contralateral side of the light-exposed retina, photoreceptor outer segments were still preserved and no invasion of green cells was noticed in the photoreceptor layer (Figure 3D; compare also Figure 1, B and C).

To analyze specifically the retinal localization and activation pattern of microglial cells, CX3CR1^{-/-} mice were analyzed by confocal laser scanning microscopy. In control non-exposed retinas, the resting microglia showed a dense network of fine arborizations of their processes in the nerve fiber layer, the inner plexiform layer and in the outer plexiform layer (Figure 4, A–C). One day after light exposure, a remarkable migration of microglial cells from the nerve fiber layer and the inner plexiform layer into the outer plexiform layer, close to the region of damage

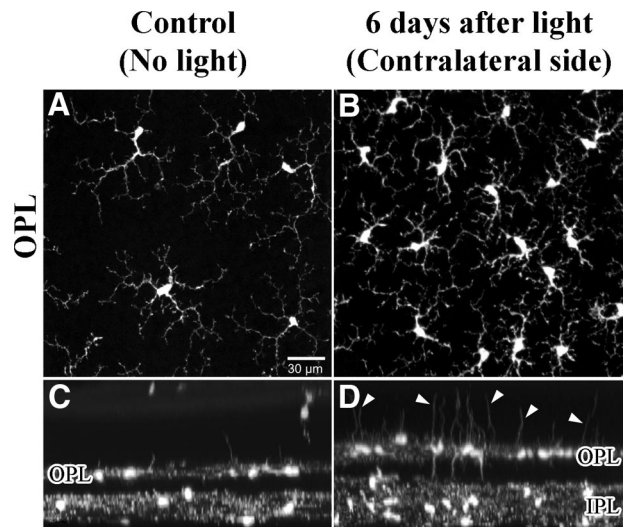


Figure 5. Confocal light micrographs of CX3CR1^{-/-} control retinas and 6 days after light exposure. **A and C:** Controls. **A:** View onto flat mount of the OPL. **C:** The same retinal area as shown in **A**, but tilted by 90°. In control retinas, microglial cells of the OPL showed characteristic arborizations of their processes and only few processes extending toward the photoreceptor layer (outer nuclear layer). **B and D:** In the contralateral retinal area from the light-exposed eye, a significant increase in number of microglial cells occurred 6 days after light exposure with a remarkable increase of thickened processes extending toward the photoreceptor layer (**arrowheads** in **D**).

occurred (Figure 4, D–G). Microglial cells within the outer plexiform layer above the hot spot became rounded and amoeboid with fewer processes, thereby displaying signs of phagocytosis (Figure 4F, arrow). Within the hot spot, the majority of microglial cells were indistinguishable from macrophages (Figure 4G). Notably, an activation pattern of microglia in the entire retina occurred as seen in the contralateral undamaged retina of the light-exposed eye where increased and thickened microglial cell processes and somata were observed (Figure 4, H–J). These activated microglial cells in an unaffected retinal area possibly indicated a similar surveillance function as was shown for microglia in the normal and diseased CNS.²⁵ Additionally, a significant increase in number of cells and their processes in the inner and outer plexiform layers (about twofold) was observed at 6 days after light stress (Figure 5, Table 3). This increase might be due to local microglial proliferation. By contrast, the other eye that was not light-exposed showed no microglial reactions (data not shown). In BMC mice we observed an immigration and subsequent differentiation of GFP-labeled cells into ramified microglial cells in the retinal periphery after light exposure (data not shown). Furthermore, the number of microglial processes extending especially into the outer nuclear layer increased about ninefold (Table 3; Figure 5).

The route of entry of macrophage precursors and the exit of debris-laden macrophages were studied by electron microscopy. Electron microscopy suggested that those routes in both BMC and CX3CR1^{-/-} mice were mainly via the retinal and optic nerve vasculature (Figure 6). Monocytes were found to attach to small vessels in the area around the optic nerve (Figure 6A). Debris-containing macrophages occupied the subretinal space in the

Table 3. Quantification of Microglial Cells and of the Number of Cell Processes in Control (No Blue Light Exposure) and in the Contralateral Uninjured Retina after Light Exposure

	Microglial cells in NFL/IPL (per mm ²)	Microglial cells in OPL (per mm ²)	Number of cell processes in ONL (per mm ²)	Number of processes/microglial cell	Process length (mean in μm)
Control, unexposed	114 ± 25	114 ± 22	28 ± 30	0.27 ± 0.3	20 ± 8
Six days after blue light-contralateral side of the light-exposed eye	250 ± 59**	239 ± 89**	274 ± 100**	1.13 ± 0.5**	17 ± 9

Three visual fields in each of three animals per group (*N* = 9 per group) were evaluated in flat mount z-stacks from ganglion cell layer to pigment epithelium. Note the almost identical numbers of microglia cells in NFL/IPL and OPL. Results are presented as means ± SD.

NFL, nerve fiber layer; IPL, inner plexiform layer; OPL, outer plexiform layer; ONL, outer nuclear layer.

Statistical analysis was performed to compare data between both groups (U-test; ***P* < 0.01).

hot spot area (Figure 6B) and were also found to attach to capillary walls at the optic nerve head (Figure 6, C and D). Furthermore, occasional debris-laden macrophages were found in the process of diapedesis into a capillary of the optic nerve head (Figure 6, E and F).

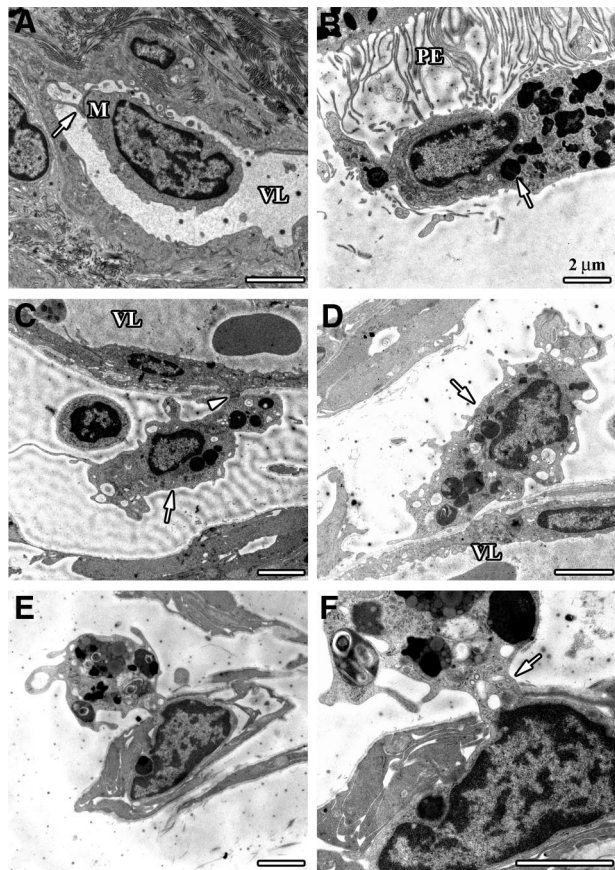


Figure 6. Electron micrographs showing debris-laden macrophages near small optic nerve vessels in BMC and CXCR1^{-/-} mice. **A:** A blood-derived monocyte (M) without any signs of phagolysosomes in close contact to an endothelial cell (arrow) in the vessel lumen (VL) of a capillary in the retrobulbar periopic nerve region. **B:** Macrophage with phagocytosed photoreceptor material (arrow) in the subretinal space at the microvilli margin of a retinal pigment epithelium cell (PE). **C and D:** Interstitial macrophages filled with debris (arrows) in close contact to basal lamina and endothelial cells. Note attachment of macrophage to endothelial cell external membrane (arrowhead). **E and F:** Macrophage with engulfed photoreceptor debris in the process of diapedesis through an optic nerve head capillary, the cell nucleus is inside the capillary whereas parts of the debris-containing cytoplasm is still externally located (arrow).

Specific Cytokines/Chemokines Are Strongly Up-Regulated after Blue Light Exposure in Retinas and Eyecups of Wild-Type Mice

Cytokine and chemokine mRNA expression profiles were monitored in the entire isolated retina, including the hot spot region and undamaged periphery, and in the eyecups, including the retinal pigment epithelium, choroid and sclera, of wild-type mice (Figure 7). *Ccl4* was signif-

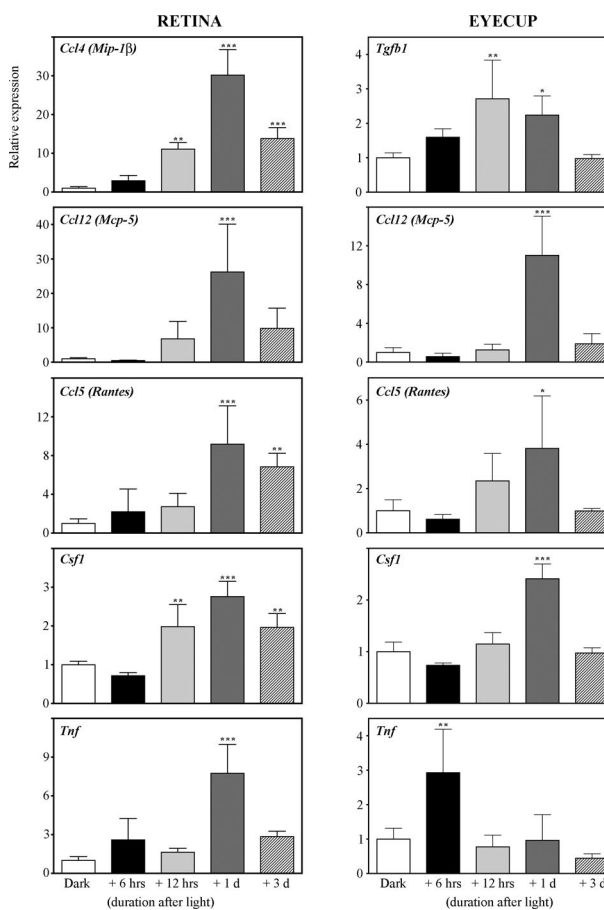


Figure 7. Chemokine/cytokine mRNA profiles in isolated retinas and eyecups of wild-type mice. Entire retinas (hot spot and periphery) and eyecups (retinal pigment epithelium, choroid, and sclera) from wild-type mice were collected after dark adaptation and at different time points after blue light exposure as indicated. Statistical analysis was performed to compare data between dark control and the different time points after light exposure in wild-type mice (**P* < 0.05, ***P* < 0.01, ****P* < 0.001).

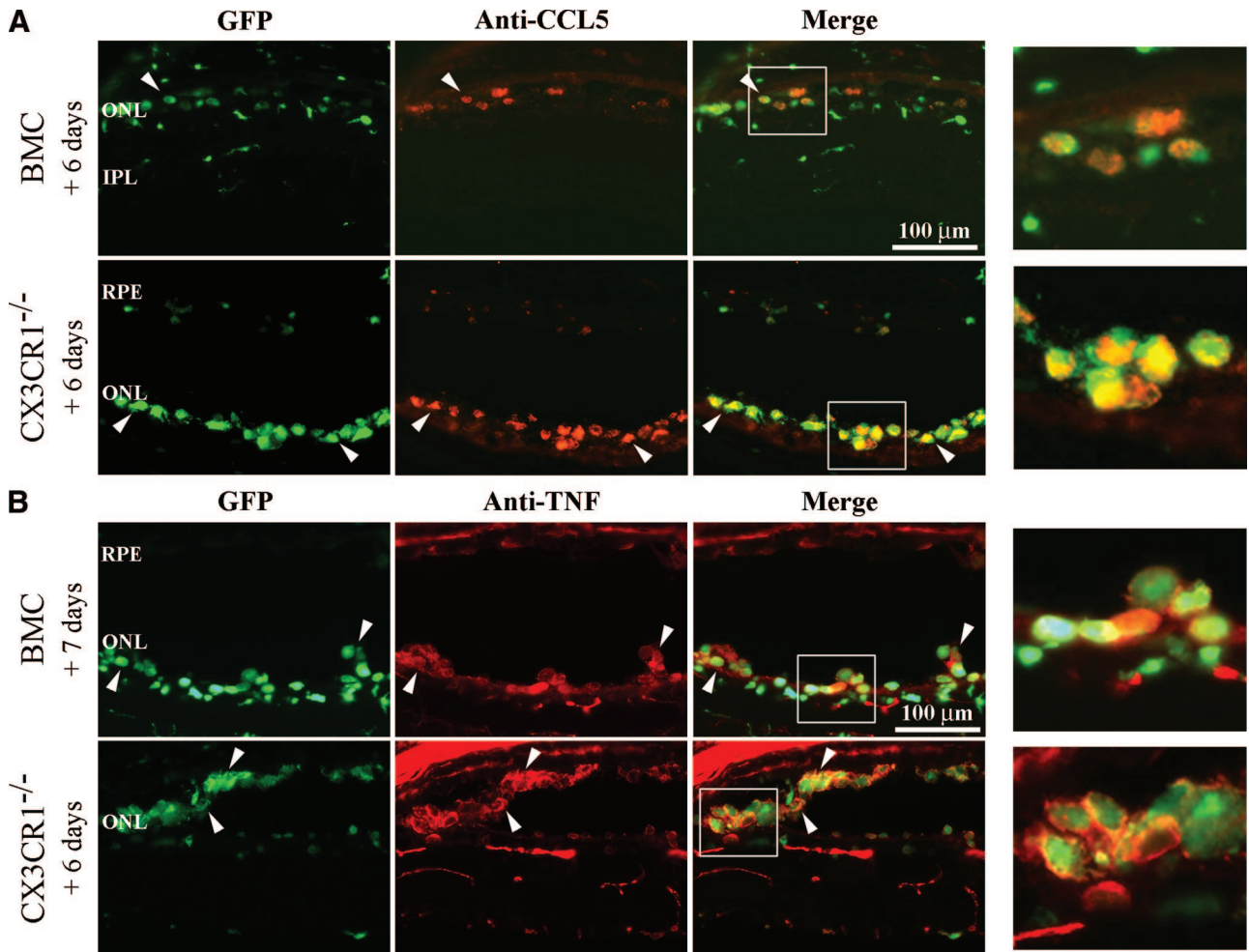


Figure 8. Cellular localization of CCL5 and TNF in retinas of BMC and CX3CR1^{-/-} mice after light exposure. **A:** CCL5 (RANTES) was expressed in a subpopulation of the invading macrophages from BMC and nearly all macrophages from CX3CR1^{-/-} mice at 6 days after light (arrowheads). **B:** A distinct expression of TNF was seen in subpopulations of macrophages from both BMC and CX3CR1^{-/-} mice (arrowheads). Scale bar = 100 μ m; 16.7 μ m for inset.

icantly overexpressed in the retinal tissue but not in the eyecup of wild-type mice 1 day after blue light exposure (Figure 7). In both tissues, *Ccl12*, *Ccl5*, and *Csf1* were highly and significantly induced after 1 day but always at a lesser extent in the eyecup (Figure 7). *Tnf* presented a pattern of activation different in retinas and eyecups. Indeed, the peak of activation for *Tnf* occurred after 1 day in the retina while *Tnf* significantly rose already at 6 hours after light exposure in the eyecup and declined rapidly thereafter, suggesting that it might constitute one of the initial attraction/activation signals for immune cells (Figure 7). The anti-inflammatory cytokine *Tgfb1* was specifically expressed in the eyecup and peaked at 12 hours followed by a gradual decline thereafter. Gene expression of other chemokines such as *Ccl9*, *Il1b*, *Cx3cl1*, *Ccl2* and *Igf1* have also been tested but they were not significantly changed in retina and eyecup of wild-type mice after light exposure compared with dark control mice (data not shown).

To show the cellular localization of CCL5 and TNF proteins, immunostainings were performed on retinal cryosections of BMC mice and of CX3CR1^{-/-} mice 6 days after light exposure (Figure 8). TNF was chosen for its roles as

the classical inflammatory mediator and initiator of oxidative stress as well as for sustaining macrophage responses. We selected CCL5 because of a specific function to promote leukocyte transendothelial migration in the retina²⁶ and macrophage modulation in other tissues.²⁷

In both strains of mice, CCL5 staining (in red) was specifically localized in GFP-positive cells, suggesting that CCL5 was expressed by macrophages within the hot spot region (Figure 8A). Similarly, TNF (in red) was detected in the cytoplasm and the perinuclear region of GFP-positive cells in BMC and in CX3CR1^{-/-} mice (Figure 8B). In contrast to the early rise of TNF in the eyecup preparation, this cellular response was observed at the peak period of macrophage activity in the retina. Thus the expression pattern of both CCL5 and TNF in the retina may be considered as a self-sustaining inflammatory response.

Discussion

We used two distinct animal models to investigate whether hematogenous immigrants or local microglia or both participate in phagocytosis after retinal injury. We

observed a distinct and rapid immigration of bone marrow-derived cells to the site of retinal injury. Likewise, resting retinal microglia was rapidly activated and migrated toward the lesion, adapted amoeboid shape and transformed into phagocytic cells. A fraction of phagocytes of either origin (blood-borne or microglia-derived) showed characteristics of both hematogenous macrophages and retinal microglia, as demonstrated by immunofluorescence staining. Particularly striking was the microglia activation pattern in the entire retina outside of the hot spot: cells increased in number and in the outer plexiform layer developed significantly more and thicker processes, which were mainly oriented toward the photoreceptors. Microglia in the unexposed eye remained unstimulated. Thus, in contrast to bone marrow-derived macrophages, microglia is "alerted" in the entire retina of the light-exposed eye and may thus critically modify neurons via specific signaling. Macrophages loaded with photoreceptor debris appeared to leave the retina via optic nerve head vessels in both BMC and CX3CR1^{-/-} mice. Autofluorescent cells in choroidal vessels of light-exposed CX3CR1^{-/-} mice as well as macrophages filled with photoreceptor debris and showing a positive staining for rhodopsin (fluorescence microscopy), entering into optic nerve head vessels (electron micrographs), supported this notion.

Bone Marrow Chimeric Mice

Whole body irradiation of mice did not induce any overt ocular and retinal changes during the period of our experiments, confirming observations previously reported.²⁸ Circulating blood monocytes give rise to tissue-resident macrophages, CNS microglia and dendritic cells. Monocytes originate from myeloid precursors and are released into the peripheral blood circulating there for several days before they replenish tissue macrophages.²⁹ A special subset of blood monocytes is destined as microglia precursor cell.³⁰

Recruitment of bone marrow-derived cells into the retina has been observed after different stimuli including retinal lesions³¹⁻³³ and inherited retinal degeneration.¹⁴ By contrast, in normal unstimulated eyes there is rather slow turnover of microglia with replacement by bone marrow-derived precursor cells in the range of 6 to 12 months.³⁴ In our study, the interval between bone marrow transplantation and light exposure was 6–8 weeks. In line with this we did not observe GFP-positive cells in dark-adapted retinal tissue but mainly in the choroidal-, ciliary- and optic nerve meningeal vasculature. In our study, light-induced retinal damage triggered an extensive immigration of GFP-expressing bone marrow cells into the area of the hot spot beginning at 6 hours and increasing significantly at 24 hours, 3 days, and 6 days after light exposure. Immigration occurred via the optic nerve and ciliary body vasculature. GFP-labeled cells showed different antibody-staining patterns underscoring heterogeneity of cell populations (Figure 2, C and D; Figure 3, B and D).

Recruitment of bone marrow-derived cells might require several signaling steps: the mobilization of mono-

cytes from bone marrow and blood, the trafficking across the blood-retina and blood-aqueous barriers including adhesion and diapedesis, the attraction to the site of injury within the retina and finally the transformation into active macrophages. Monocyte recruitment is regulated by members of the chemokine family of chemotactic cytokines. In mice, the CC chemokine receptor 2 (CCR2) was shown to be highly expressed on blood monocytes and implicated in the recruitment of monocytes. In addition, the ligands *Ccl2* and *Ccl7* were critical for monocyte mobilization from bone marrow¹⁸ and *Ccl5* supported transepithelial migration in the retina.²⁶ In our study, *Ccl12* rather than *Ccl2* was significantly up-regulated after light exposure underscoring different regulative mechanisms in different conditions.

Inflammatory Signaling in Wild-Type Mice

Inflammatory signaling comprises a vast array of cytokines and chemokines. Some of them, which were found to be increased in many other studies of brain and retina, did not reveal a blue light-evoked expression pattern in our study (not shown). For example, in retinal degeneration (*rd1* mouse), *Ccl2*, *Ccl7*, *Ccl3*, *Ccl4*, and *Ccl5* were up-regulated during the period of most severe photoreceptor loss concomitant with microglia activity.³⁵ In our study, retinal RNA-inflammatory chemokine expression peaked at 1 day after light exposure and declined thereafter, whereas morphological lesions and macrophage activity were greatest at 3 days and 6 days after light exposure. In the eyecup, *Tnf* rapidly peaked already at 6 hours after light and may therefore constitute an initial attraction and activation signal for blood-borne cells. *Csf1* began to rise at 12 hours after light in the retina and might thus activate or regulate local resident microglia. Similarly, *Tgfb1* was distinctly up-regulated in the eyecup but not in the retina, beginning at 6 hours and peaking at 12 hours after light and could thus represent a protective anti-inflammatory response of the pigment epithelium.

CX3CR1^{-/-} Mice

Microglia is the local phagocytic system of the CNS including the retina. In the brain, microglia can act as antigen presenting cell and may be neurotoxic as well as neuroprotective under various experimental conditions.¹⁹ The chemokine system plays an essential role not only in leukocyte trafficking but also in immunity.³⁶ The fractalkine chemokine (CX3CL1) is unique in that it is the only ligand for only one receptor, the CX3CR1, in the brain. Fractalkine was shown to have several functions, especially the regulation of microglia neurotoxicity,¹¹ the transmission of pathological pain³⁷ and neuron to glia signaling.³⁸

Because CX3CR1 is expressed on CNS microglia, this fact was used to create a mouse model for selectively labeling brain microglia.⁸ We used this mouse model to study microglia behavior and to differentiate between acutely immigrated monocyte-macrophages and glia-derived macrophages in the retina after acute light damage.

In the brain, complete deficiency of the fractalkine receptor (CX3CR1^{-/-}) resulted in insufficient migration of microglia and in an increase in microglia neurotoxicity by worsening neurodegeneration.¹¹ In our study, light-induced degeneration was not enhanced in CX3CR1^{-/-} mice and homo- and heterozygous knockout mice were practically indistinguishable in damage severity. Similarly, recruitment of retinal microglia in the young mouse eye was CX3CR1-independent.³⁹ Furthermore, *Cx3cl1* mRNA was not up-regulated after light exposure (data not shown). However, posttranslational regulation of protein levels has been described in the brain³⁶ and cannot be excluded in our study. Effects of *Cx3cr1* deficiency in microglial activation may thus depend on the nature of the stimulus and possibly on species and strain differences. In the retina, activation and migration of microglia toward the region of injury was induced by a variety of conditions, including different levels of white light or laser and axotomy of one optic nerve,⁴⁰⁻⁴³ retinal degeneration,^{9,35} docosahexaenoic acid hydroperoxide,⁴⁴ retinal detachment⁴⁵ and ischemia-induced retinopathy.⁴⁶

However, molecular signaling by activated microglia and the effects of activation have not been investigated in detail for the retina. Brain microglia can be activated, for example, by pro-inflammatory signals and by neuron damage.¹⁰ Pattern recognition receptors on microglia can monitor a large variety of damaging agents resulting in migration and phagocytic activity as well as in the release of inflammatory messengers (cytokines, chemokines and lipid mediators) and reactive oxygen species, which collectively lead to neurotoxicity.¹⁰ Similar mechanisms may exist in the retina. Apoptosis, release of inflammatory lipid mediators and reactive oxygen species are known to occur in retinal light damage^{1,2,47} and may thus act as initial local signals for microglia activation.

Neuron-glia cross-talk may not only comprise death signals from dead neurons or activated microglia but also rescue mechanisms. In the retina, activated microglia expressed neurotrophic factors, which were found to signal to Müller cells that in turn released fibroblast growth factor 2 and glial cell line-derived neurotrophic factor and thus were suggested to represent a rescue mechanism in light-induced retinal degeneration.¹³ Brain microglia also expresses purinoceptors, which are activated by ATP, UTP, and UDP as ligands.⁴⁸⁻⁵⁰ Since ATP is abundantly produced and used in the retina, a similar mechanism could be used for retinal microglia activation.

Microglia in Retinal Degeneration

Retinal microglia may fulfill important functions that go beyond the mere removal of dead photoreceptor and/or pigment epithelial cells. It is noteworthy that in our study microglia distinctly increased in number and developed pronounced processes in the entire retina outside of the hot spot, which may indicate similar survey functions as were described for the normal and injured brain.^{25,48} In addition, activated microglia from the contralateral side of the light-exposed eye may help to replenish microglia in the damaged retinal area apart from the slow, regular

substitution by blood monocytes. The survey activity may convey the message of cell death already at early stages of degeneration with ensuing remodeling of inner retinal architecture and wiring. As in other brain degenerations, such deafferentiation by photoreceptor cell death can induce distinct remodeling.⁵¹ Retinal remodeling gains increasing importance in view of therapeutic regimens for retinitis pigmentosa including gene therapy, chip implantation, stem cell and other tissue transplantation. Remodeling in its early stage may allow some of the experimental therapies to succeed.^{52,53} Thus it will be important to analyze activity patterns of retinal microglia in early stages of diseases, including age-related macular degeneration.

Subretinal Deposits

SLO with indocyanine green angiography revealed no leakage of fluid from retinal vessels (Figure 1). However, a subretinal edema was apparent at 24 hours after light and resolved within 6 to 7 days after exposure. A recent study investigated the interaction of proinflammatory cytokines/chemokines and fluid transport.⁵⁴ A similar mechanism may regulate the relatively rapid removal of subretinal edema after acute light-induced lesion in our study.

Confirming fluorescence microscopy, GFP-labeled cells remained in the retina for extended periods of time. Notably, an accumulation of subretinal and/or pigment epithelial material absorbing at 488 nm appeared in the hot spot in both wild-type and BMC mice. This absorption would coincide with that of retinoid components derived from the visual pigment chromophore 11-*cis*-retinal in photoreceptor outer segments. In addition, material absorbing at 795 nm was monitored, again in both wild-type and BMC mice, which would not match the known retinoid spectrum and thus needs to be analyzed further.

Conclusion

A strong, acute retinal lesion evokes both the rapid recruitment of bone marrow-derived macrophages and of activated resident microglia to the focus of injury. There are distinct differences, however, in the activation pattern of both cell populations: whereas bone marrow-derived cells concentrate in the focus of damage, microglia is "on alarm" in the entire retina of the light-exposed eye. CX3CR1 deficiency did not alter the damage pattern in our study indicating that this ligand-receptor system may be replaced by redundant mechanisms or is not required in acute retinal injury. Macrophages loaded with photoreceptor debris appeared to leave the retina into the general circulation and may enter the spleen, a process that would enable an immunization against retinal proteins.⁴ Specific retinal proteins have long been used to induce ocular autoimmune inflammation.⁵⁵ Future studies need to elucidate molecular signals regulating monocyte and microglia activation patterns and the potential for autoimmune reactions after injury leading to or enhancing retinal degenerations.

Acknowledgments

The expert technical assistance of Coni Imsand, Philipp Huber, and Hedi Wariwoda is gratefully acknowledged.

References

1. Remé CE: The dark side of light: rhodopsin and the silent death of vision the proctor lecture. *Invest Ophthalmol Vis Sci* 2005, 46:2671–2682
2. Wenzel A, Grimm C, Samardzija M, Remé CE: Molecular mechanisms of light-induced photoreceptor apoptosis and neuroprotection for retinal degeneration. *Prog Retin Eye Res* 2005, 24:275–306
3. Streilein JW: Ocular immune privilege: the eye takes a dim but practical view of immunity and inflammation. *J Leukoc Biol* 2003, 74:179–185
4. Niederhorn JY: See no evil, hear no evil, do no evil: the lessons of immune privilege. *Nat Immunol* 2006, 7:354–359
5. Hoppeler T, Hendrickson P, Dietrich C, Remé C: Morphology and time-course of defined photochemical lesions in the rabbit retina. *Curr Eye Res* 1988, 7:849–860
6. Joly S, Samardzija M, Wenzel A, Thiersch M, Grimm C: Nonessential role of $\beta 3$ and $\beta 5$ integrin subunits for efficient clearance of cellular debris after light-induced photoreceptor degeneration. *Invest Ophthalmol Vis Sci* 2009, 50:1423–1432
7. Lang KS, Recher M, Junt T, Navarini AA, Harris NL, Freigang S, Odermatt B, Conrad C, Ittner LM, Bauer S, Luther SA, Uematsu S, Akira S, Hengartner H, Zinkernagel RM: Toll-like receptor engagement converts T-cell autoreactivity into overt autoimmune disease. *Nat Med* 2005, 11:138–145
8. Jung S, Aliberti J, Graemmel P, Sunshine MJ, Kreutzberg GW, Sher A, Littman DR: Analysis of fractalkine receptor CX3CR1 function by targeted deletion and green fluorescent protein reporter gene insertion. *Mol Cell Biol* 2000, 20:4106–4114
9. Gupta N, Brown KE, Milam AH: Activated microglia in human retinitis pigmentosa, late-onset retinal degeneration, and age-related macular degeneration. *Exp Eye Res* 2003, 76:463–471
10. Block ML, Zecca L, Hong JS: Microglia-mediated neurotoxicity: uncovering the molecular mechanisms. *Nat Rev Neurosci* 2007, 8:57–69
11. Cardona AE, Piro EP, Sasse ME, Kostenko V, Cardona SM, Dijkstra IM, Huang D, Kidd G, Dombrowski S, Dutta R, Lee JC, Cook DN, Jung S, Lira SA, Littman DR, Ransohoff RM: Control of microglial neurotoxicity by the fractalkine receptor. *Nat Neurosci* 2006, 9:917–924
12. Srinivasan B, Roque CH, Hempstead BL, Al-Ubaidi MR, Roque RS: Microglia-derived proinflammatory growth factor promotes photoreceptor cell death via p75 neurotrophin receptor. *J Biol Chem* 2004, 279:41839–41845
13. Harada T, Harada C, Kohsaka S, Wada E, Yoshida K, Ohno S, Mamada H, Tanaka K, Parada LF, Wada K: Microglia-Müller glia cell interactions control neurotrophic factor production during light-induced retinal degeneration. *J Neurosci* 2002, 22:9228–9236
14. Sasahara M, Otani A, Oishi A, Kojima H, Yodoi Y, Kameda T, Nakamura H, Yoshimura N: Activation of bone marrow-derived microglia promotes photoreceptor survival in inherited retinal degeneration. *Am J Pathol* 2008, 172:1693–1703
15. Jha P, Bora PS, Bora NS: The role of complement system in ocular diseases including uveitis and macular degeneration. *Mol Immunol* 2007, 44:3901–3908
16. Hollyfield JG, Bonilha VL, Rayborn ME, Yang X, Shadrach KG, Lu L, Ufret RL, Salomon RG, Perez VL: Oxidative damage-induced inflammation initiates age-related macular degeneration. *Nat Med* 2008, 14:194–198
17. Combadiere C, Feumi C, Raoul W, Keller N, Rodero M, Pezard A, Lavalette S, Houssier M, Jonet L, Picard E, Debre P, Sirinyan M, Deterre P, Ferroukhi T, Cohen SY, Chauvaud D, Jeanny JC, Chemtob S, Behar-Cohen F, Sennlaub F: CX3CR1-dependent subretinal microglia cell accumulation is associated with cardinal features of age-related macular degeneration. *J Clin Invest* 2007, 117:2920–2928
18. Tsou CL, Peters W, Si Y, Slaymaker S, Aslanian AM, Weisberg SP, Mack M, Charo IF: Critical roles for CCR2 and MCP-3 in monocyte mobilization from bone marrow and recruitment to inflammatory sites. *J Clin Invest* 2007, 117:902–909
19. Ambrosini E, Aloisi F: Chemokines and glial cells: a complex network in the central nervous system. *Neurochem Res* 2004, 29:1017–1038
20. Haak S, Croxford AL, Kreyborg K, Heppner FL, Pouly S, Becher B, Waisman A: IL-17A and IL-17F do not contribute vitally to autoimmune neuro-inflammation in mice. *J Clin Invest* 2009, 119:61–69
21. Grimm C, Wenzel A, Williams T, Rol P, Hafezi F, Remé C: Rhodopsin-mediated blue-light damage to the rat retina: effect of photoreversal of bleaching. *Invest Ophthalmol Vis Sci* 2001, 42:497–505
22. Breton ME, Schueller AW, Lamb TD, Pugh EN Jr: Analysis of ERG a-wave amplification and kinetics in terms of the G-protein cascade of phototransduction. *Invest Ophthalmol Vis Sci* 1994, 35:295–309
23. Seeliger MW, Beck SC, Pereyra-Munoz N, Dangel S, Tsai JY, Luhmann UF, van de Pavert SA, Wijnholds J, Samardzija M, Wenzel A, Zrenner E, Narfstrom K, Fahl E, Tanimoto N, Acar N, Tonagel F: In vivo confocal imaging of the retina in animal models using scanning laser ophthalmoscopy. *Vision Res* 2005, 45:3512–3519
24. Thiersch M, Raffelsberger W, Frigg R, Samardzija M, Wenzel A, Poch O, Grimm C: Analysis of the retinal gene expression profile after hypoxic preconditioning identifies candidate genes for neuroprotection. *BMC Genomics* 2008, 9:73
25. Nimmerjahn A, Kirchhoff F, Helmchen F: Resting microglial cells are highly dynamic surveillants of brain parenchyma in vivo. *Science* 2005, 308:1314–1318
26. Crane JJ, Xu H, Wallace C, Manivannan A, Mack M, Liversidge J, Marquez G, Sharp PF, Forrester JV: Involvement of CCR5 in the passage of Th1-type cells across the blood-retina barrier in experimental autoimmune uveitis. *J Leukoc Biol* 2006, 79:435–443
27. Li Z, Xia F, Zhang Y: Polarized release of RANTES by cytotoxic T cells paints tumor targets and enhances apoptotic cell removal. *FASEB J* 2008, 22:1748–1755
28. Igarashi T, Miyake K, Hayakawa J, Kawabata K, Ishizaki M, Takahashi H, Shimada T: Apoptotic cell death and regeneration in the newborn retina after irradiation prior to bone marrow transplantation. *Curr Eye Res* 2007, 32:543–553
29. Gordon S, Taylor PR: Monocyte and macrophage heterogeneity. *Nat Rev Immunol* 2005, 5:953–964
30. Tacke F, Randolph GJ: Migratory fate and differentiation of blood monocyte subsets. *Immunobiology* 2006, 211:609–618
31. Kaneko H, Nishiguchi KM, Nakamura M, Kachi S, Terasaki H: Characteristics of bone marrow-derived microglia in the normal and injured retina. *Invest Ophthalmol Vis Sci* 2008, 49:4162–4168
32. Caicedo A, Espinosa-Heidmann DG, Pina Y, Hernandez EP, Cousins SW: Blood-derived macrophages infiltrate the retina and activate Müller glial cells under experimental choroidal neovascularization. *Exp Eye Res* 2005, 81:38–47
33. Chan-Ling T, Baxter L, Afzal A, Sengupta N, Caballero S, Rosinova E, Grant MB: Hematopoietic stem cells provide repair functions after laser-induced Bruch's membrane rupture model of choroidal neovascularization. *Am J Pathol* 2006, 168:1031–1044
34. Albin TA, Wang RC, Reiser B, Zamir E, Wu GS, Rao NA: Microglial stability and repopulation in the retina. *Br J Ophthalmol* 2005, 89:901–903
35. Zeng HY, Zhu XA, Zhang C, Yang LP, Wu LM, Tso MO: Identification of sequential events and factors associated with microglial activation, migration, and cytotoxicity in retinal degeneration in rd mice. *Invest Ophthalmol Vis Sci* 2005, 46:2992–2999
36. Ransohoff RM, Liu L, Cardona AE: Chemokines and chemokine receptors: multipurpose players in neuroinflammation. *Int Rev Neurobiol* 2007, 82:187–204
37. Milligan ED, Sloane EM, Watkins LR: Glia in pathological pain: A role for fractalkine. *J Neuroimmunol* 2008, 198:113–120
38. Pocock JM, Kettenmann H: Neurotransmitter receptors on microglia. *Trends Neurosci* 2007, 30:527–535
39. Kezic J, Xu H, Chinnery HR, Murphy CC, McMenamin PG: Retinal microglia and uveal tract dendritic cells and macrophages are not CX3CR1 dependent in their recruitment and distribution in the young mouse eye. *Invest Ophthalmol Vis Sci* 2008, 49:1599–1608
40. Ng TF, Streilein JW: Light-induced migration of retinal microglia into the subretinal space. *Invest Ophthalmol Vis Sci* 2001, 42:3301–3310
41. Zhang C, Shen JK, Lam TT, Zeng HY, Chiang SK, Yang F, Tso MO: Activation of microglia and chemokines in light-induced retinal degeneration. *Mol Vis* 2005, 11:887–895
42. Eter N, Engel D, Meyer L, Helb HM, Roth F, Maurer J, Holz FG, Kurts C: In vivo visualization of dendritic cells, macrophages and microglial

- cells responding to laser-induced damage in the fundus of the eye. *Invest Ophthalmol Vis Sci* 2008, 49:3649–3658
43. Thanos S: Sick photoreceptors attract activated microglia from the ganglion cell layer: a model to study the inflammatory cascades in rats with inherited retinal dystrophy. *Brain Res* 1992, 588:21–28
 44. Saraswathy S, Wu G, Rao NA: Retinal microglial activation and chemotaxis by docosahexaenoic acid hydroperoxide. *Invest Ophthalmol Vis Sci* 2006, 47:3656–3663
 45. Nakazawa T, Hisatomi T, Nakazawa C, Noda K, Maruyama K, She H, Matsubara A, Miyahara S, Nakao S, Yin Y, Benowitz L, Hafezi-Moghadam A, Miller JW: Monocyte chemoattractant protein 1 mediates retinal detachment-induced photoreceptor apoptosis. *Proc Natl Acad Sci USA* 2007, 104:2425–2430
 46. Davies MH, Eubanks JP, Powers MR: Microglia and macrophages are increased in response to ischemia-induced retinopathy in the mouse retina. *Mol Vis* 2006, 12:467–477
 47. Jung H, Remé C: Light-evoked arachidonic acid release in the retina: illuminance/duration dependence and the effects of quinacrine, melittin and lithium: light-evoked arachidonic acid release. *Graefes Arch Clin Exp Ophthalmol* 1994, 232:167–175
 48. Davalos D, Grutzendler J, Yang G, Kim JV, Zuo Y, Jung S, Littman DR, Dustin ML, Gan WB: ATP mediates rapid microglial response to local brain injury in vivo. *Nat Neurosci* 2005, 8:752–758
 49. Haynes SE, Hoppel G, Yang G, Kurpius D, Dailey ME, Gan WB, Julius D: The P2Y₁₂ receptor regulates microglial activation by extracellular nucleotides. *Nat Neurosci* 2006, 9:1512–1519
 50. Koizumi S, Shigemoto-Mogami Y, Nasu-Tada K, Shinozaki Y, Ohsawa K, Tsuda M, Joshi BV, Jacobson KA, Kohsaka S, Inoue K: UDP acting at P2Y₆ receptors is a mediator of microglial phagocytosis. *Nature* 2007, 446:1091–1095
 51. Marc RE, Jones BW, Watt CB, Strettoi E: Neural remodeling in retinal degeneration. *Prog Retin Eye Res* 2003, 22:607–655
 52. Lee JE, Liang KJ, Fariss RN, Wong WT: Ex vivo dynamic imaging of retinal microglia using time-lapse confocal microscopy. *Invest Ophthalmol Vis Sci* 2008, 49:4169–4176
 53. Lewis GP, Sethi CS, Carter KM, Charteris DG, Fisher SK: Microglial cell activation following retinal detachment: a comparison between species. *Mol Vis* 2005, 11:491–500
 54. Shi GMA, Banzon T, Jalickee S, Li R, Hammer J, Miller SS: Control of chemokine gradients by the retinal pigment epithelium. *Invest Ophthalmol Vis Sci* 2008, 49:4620–4630
 55. Caspi RR: Ocular autoimmunity: the price of privilege? *Immunol Rev* 2006, 213:23–35
 56. Hicks DBC: Different rhodopsin monoclonal antibodies reveal different binding patterns on developing and adult rat retina. *J Histochem Cytochem* 1987, 35:1317–1328